

MEMBRANES

Ion-capture electro dialysis using multifunctional adsorptive membranes

Adam A. Uliana^{1,2}, Ngoc T. Bui^{2,3}†, Jovan Kamcev⁴‡, Mercedes K. Taylor^{2,4,5}, Jeffrey J. Urban^{2,3}, Jeffrey R. Long^{1,2,4*}

Technologies that can efficiently purify nontraditional water sources are needed to meet rising global demand for clean water. Water treatment plants typically require a series of costly separation units to achieve desalination and the removal of toxic trace contaminants such as heavy metals and boron. We report a series of robust, selective, and tunable adsorptive membranes that feature porous aromatic framework nanoparticles embedded within ion exchange polymers and demonstrate their use in an efficient, one-step separation strategy termed ion-capture electro dialysis. This process uses electro dialysis configurations with adsorptive membranes to simultaneously desalinate complex water sources and capture diverse target solutes with negligible capture of competing ions. Our methods are applicable to the development of efficient and selective multifunctional separations that use adsorptive membranes.

Escalating demand for water in agriculture, energy, industry, and municipal sectors, coupled with limited natural freshwater, necessitates the rapid development of technologies that will enable access to clean water from alternative sources (1). Nontraditional water sources, such as wastewater, brackish water, or seawater, could provide abundant water globally, but these complex solutions contain high salt concentrations and trace toxic ions (such as heavy metals and oxyanions), which vary by location and type of water source (2–4). At the same time, nontraditional water sources often contain high-value ions (for example, uranium in seawater and precious metals and nutrients in wastewater), but current technologies lack the efficiency and selectivity needed for their cost-effective extraction (5, 6). Electro dialysis, membrane capacitive deionization, and reverse osmosis are among the most common membrane-based technologies used for removing ions from water (2, 4). However, these approaches are incapable of selectively isolating individual solutes, and toxic ions are instead returned to the environment with the concentrated brine solutions (2). Accordingly, developing membrane technologies with substantially improved selectivity for either water desalination or the recovery of individual ions

or molecules from water is considered one of the most important objectives in the separations industry (3–5, 7, 8).

Adsorptive membranes are an emerging class of materials that have been shown to exhibit improved performance in numerous separations when compared with conventional

membranes, including for water purification (4, 9–13). However, improvements are needed in the capacities, selectivities, and regenerabilities achievable with these materials to enable their wide-scale use, which is also currently hindered by the limited structural and chemical tunability of most adsorptive membranes (4). We therefore sought to develop a highly modular adsorptive membrane platform for use in multifunctional water-purification applications, which is based on the incorporation of porous aromatic frameworks (PAFs) into ion exchange membranes. Built of organic nodes and aromatic linkers, PAFs have high-porosity diamondoid structures with pore morphologies and chemical affinities that can be tuned through the choice of node and linker (Fig. 1, A and B) (14, 15). Densely functionalized PAFs exhibit among the highest selectivities, capacities, and uptake kinetics for the capture of Hg^{2+} (16), Nd^{3+} (17), Cu^{2+} (18), Pb^{2+} (19), UO_2^{2+} (20, 21), $\text{B}(\text{OH})_3$ (22), Fe^{3+} (23), and AuCl_4^- (24) from water. In contrast to typical inorganic or hybrid adsorbent fillers, such as metal-organic frameworks (25), PAFs also have extraordinary hydrothermal stability (15) and chemical compositions that should facilitate incorporation into polymer membranes. However, there are

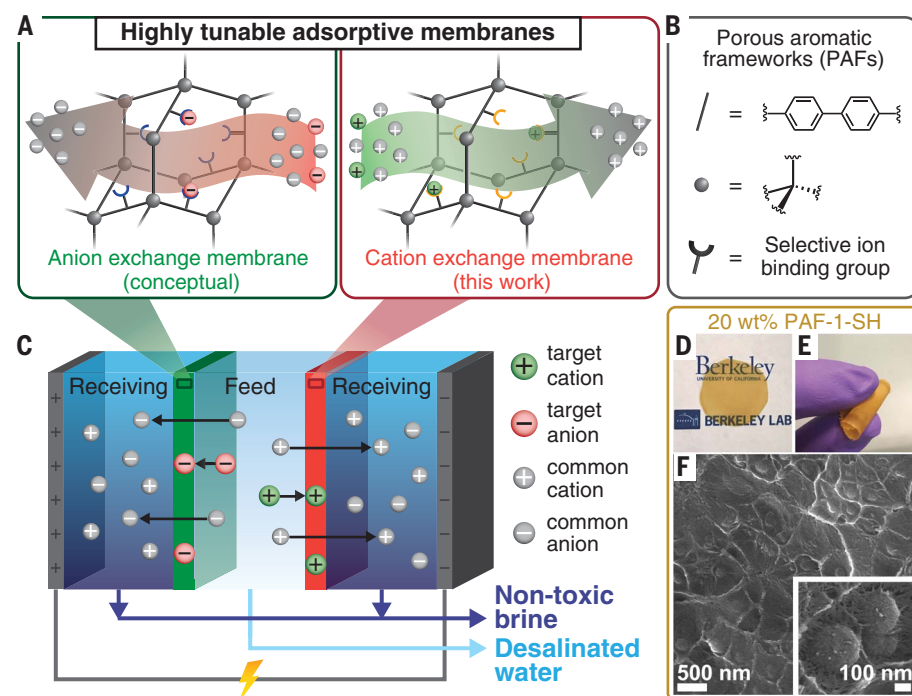


Fig. 1. Design of composite membranes and application in ion-capture electro dialysis (IC-ED). (A and B) Tunable composite membranes were prepared by embedding PAFs with selective ion binding sites into cation exchange polymer matrices. (C) We demonstrate the use of these adsorptive membranes in an electro dialysis-based process for the selective capture of target cations (right-hand side) from water and simultaneous desalination. Water splitting occurs at both electrodes to maintain electroneutrality. (D and E) PAF-embedded membranes are defect-free and exhibit optical transparency and high flexibility. (F) Cross-sectional scanning electron micrographs (expanded view in inset) revealed high PAF dispersibility and strong, favorable interactions between the PAF and polymer matrix.

¹Department of Chemical and Biomolecular Engineering, University of California, Berkeley, CA 94720, USA. ²Materials Sciences Division, Lawrence Berkeley National Laboratory, Berkeley, CA 94720, USA. ³The Molecular Foundry, Lawrence Berkeley National Laboratory, Berkeley, CA 94720, USA. ⁴Department of Chemistry, University of California, Berkeley, CA 94720, USA. ⁵Center for Integrated Nanotechnologies, Sandia National Laboratories, Albuquerque, NM 87185, USA. *Corresponding author. Email: jrlong@berkeley.edu

†Present address: School of Chemical, Biological, and Materials Engineering and School of Civil Engineering and Environmental Science, University of Oklahoma, Norman, OK 73019, USA.

‡Present address: Department of Chemical Engineering, and Macromolecular Science and Engineering, University of Michigan, Ann Arbor, MI 48109, USA.

only few examples of PAF-incorporated membranes in the literature, with applications limited to antiaging gas-separation membranes, fiber membranes, pervaporation membranes, and thin-film layers (15, 26).

We present a class of adsorptive membranes featuring ion-selective PAF nanoparticles blended into ion exchange membranes. Target ions (Hg^{2+} , Cu^{2+} , and Fe^{3+}) in feedwater solutions are selectively captured by these adsorbent-embedded membranes, whereas competing ions (such as Na^+ and Cl^-) permeate freely (Fig. 1C). This process allows for desalination and detoxification of water, recovery of toxic or high-value target ions, and generation of nontoxic brine streams in an efficient one-step process. This proof-of-concept report focuses on the selective capture of various cationic and neutral species, but the concept can be extended to construct more complex separation schemes for simultaneous capture of target cations and anions.

Model adsorptive membranes were prepared with up to 20 wt % (44 vol %) of the Hg^{2+} -selective PAF-1-SH (16) embedded in a sulfonated polysulfone (sPSF) cation exchange matrix (60% sulfonation) (figs. S1, S6, and S7). Loadings were confirmed with thermogravimetric analysis, helium pycnometry, and N_2 gas adsorption measurements (figs. S8 and S17 and table S2). All the films exhibit substantial optical transparency, which is indicative of high PAF dispersity (Fig. 1D and fig. S2). The films are also highly flexible and can be contorted without damage (Fig. 1E and fig. S3). Dynamic light scattering and scanning electron microscopy (SEM) characterization of PAF samples before membrane incorporation revealed the presence of spherical particles with typical diameters of ~ 200 nm (figs. S15 and S16). Cross-sectional SEM images of 20 wt % PAF-1-SH membranes revealed that these particles are uniformly dispersed without agglomerations, defects, or sieve-in-a-cage morphologies (Fig. 1F and fig. S18). The uniform and robust nature of the composite membranes can be ascribed to favorable van der Waals interactions between the framework and polymer, π - π stacking, and polymer filling of the PAF mesopores (26).

Conventional charged membranes are subject to an ion permeability-selectivity trade-off, in which swelling resulting from water uptake decreases selectivity but enlarges free-volume pathways, thereby increasing permeability (27). By contrast, our composite membranes exhibit enhanced water uptake in tandem with diminished swelling, which is due to the presence of a highly porous filler that is capable of cross-linking interactions with the parent polymer (Fig. 2A). These interfacial interactions can be seen in cross-sectional SEM images (Fig. 1F, inset) and are reflected in an increase in the membrane glass transition temperature (T_g)

with increasing PAF loading (Fig. 2B). The dimensional and chemical stabilities of neat and PAF-embedded sPSF membranes were further probed by dissolution studies, in which each membrane was reimmersed in casting solvents, 12 M HCl or 12 M NaOH for 24 hours. Neat sPSF membrane samples redissolved in various casting solvents, as expected, but the abundant cross-linking interactions in membranes loaded with 20 wt % PAF-1-SH rendered them fully or partially insoluble in each solvent (fig. S20). Similarly, whereas neat sPSF membranes with ultrahigh charge densities become water soluble owing to excessive water uptake (figs. S6, S7, and S21), incorporation of 20 wt % PAF-1-SH into these highly charged matrices yields freestanding membranes that exhibit minimal swelling even after 1 year of water immersion (fig. S21 and section 2.1 of the supplementary materials).

Batch adsorption experiments revealed that up to 93% of the Hg^{2+} adsorption sites in bulk PAF-1-SH (fig. S23) remain accessible upon incorporation of 20 wt % of the framework into a sPSF membrane (Fig. 2C and table S6). A comparison of the kinetics data for the bulk framework (fig. S26) with that obtained for the neat sPSF and 20 wt % PAF-1-SH membranes (fig. S27) suggests that adsorption in the composite membrane is rate-limited by transport

through the sPSF matrix. Bulk PAF-1-SH exhibits a high affinity for Hg^{2+} over a number of competing ions and exceptional Hg^{2+} selectivity when exposed to environmental water samples (fig. S28). This selectivity stems from optimal soft acid-soft base interactions between Hg^{2+} and the thiol groups in PAF-1-SH (16) and is preserved in the 20 wt % PAF-1-SH-loaded membrane (Fig. 2D). The membrane exhibits excellent stability to adsorption-desorption cycling, with only an 8% loss in Hg^{2+} capacity over the course of 10 cycles, and the Hg^{2+} capacity remains approximately constant after three cycles.

Composite membranes with 20 wt % PAF-1-SH were evaluated for Hg^{2+} -capture electro-dialysis of synthetic groundwater, brackish water, and industrial wastewater samples with 5 parts per million (ppm) added Hg^{2+} (Fig. 3, A to C). These complex feedwater sources were chosen for their diversity in salinity levels, dissolved ions, and pH values (tables S4 and S5). For these proof-of-concept experiments, we used a custom-made, two-compartment cell with the membrane separating the feed from the receiving solution (figs. S30 to S32). Notably, the Hg^{2+} concentration in the feed solution was selectively reduced below levels detectable with inductively coupled plasma optical emission spectrometry (ICP-OES), and no Hg^{2+}

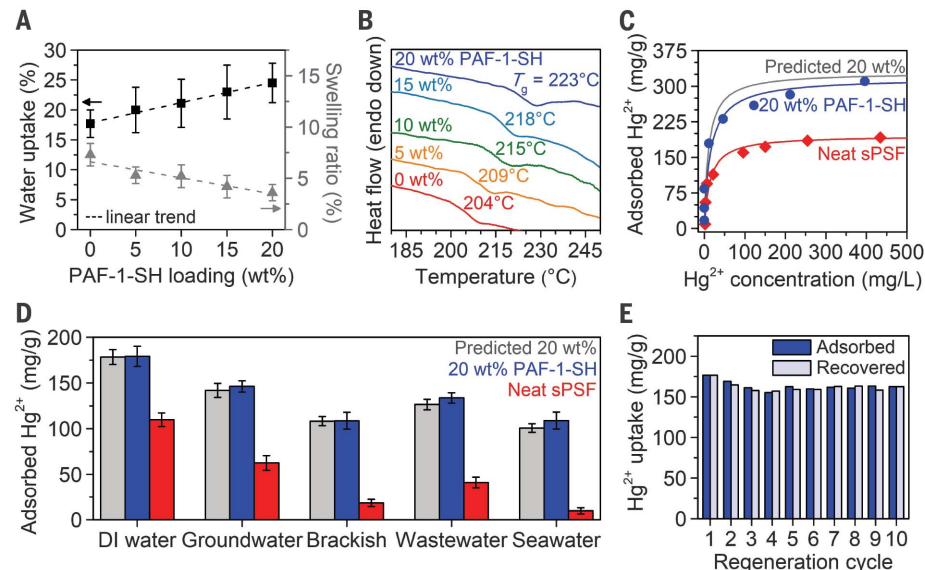


Fig. 2. Properties of PAF-embedded ion exchange membranes. (A and B) Composite membranes exhibit increasing water uptake, swelling resistance, and glass transition temperature (T_g) with increasing PAF-1-SH loading. (C) Comparison of equilibrium Hg^{2+} uptake in neat sPSF and sPSF with 20 wt % PAF-1-SH. Solid lines represent fits with a Langmuir model. Mercury ion uptake in the composite membrane closely approaches the predicted saturation uptake (329 mg/g), assuming all binding sites in the PAF particles are accessible. (D) Equilibrium uptake of Hg^{2+} in neat sPSF and sPSF with 20 wt % PAF-1-SH exposed to deionized (DI) water and various synthetic water samples with 100 ppm added Hg^{2+} . (E) Mercury ion uptake in 20 wt % PAF-1-SH membranes as a function of cycle number. Minimal decrease in Hg^{2+} uptake occurs over 10 cycles. The initial Hg^{2+} concentration was 100 ppm for each cycle, and all Hg^{2+} captured in each cycle was recovered by using HCl and NaNO_3 . Error bars denote ± 1 SD around the mean from at least three separate measurements.

was detected in the receiving solution, indicating the complete capture of Hg^{2+} during treatment of each water sample. Meanwhile, all competing cations (Na^+ , K^+ , Mg^{2+} , Ca^{2+} , Ba^{2+} , Mn^{2+} , Fe^{3+} , Ni^{2+} , Cu^{2+} , Zn^{2+} , Cd^{2+} , and Pb^{2+}) were successfully transported into the receiving solution, resulting in >97 to 99% feed desalination (Fig. 3, A to C, insets). Negligible quantities of each competing ion were captured by the membrane (figs. S37 to S43). These selective, multifunctional performances were also maintained upon integrating the PAF-1-SH membranes into a practical stack electro-dialysis device (figs. S54 to S57 and section 1.9 of the supplementary materials). By contrast, no appreciable Hg^{2+} was captured when using neat sPSF membranes (figs. S34 to S36 and S58).

Breakthrough experiments further revealed the outstanding Hg^{2+} ion-capture efficiency of the adsorptive membranes in an ion-capture electro-dialysis (IC-ED) process. Both 10 and 20 wt % PAF-1-SH membranes achieved 96% of their theoretical capacities before Hg^{2+} was first detected in the receiving solution (Fig. 3D and section 1.10 of the supplementary materials). By contrast, Hg^{2+} immediately permeated through a neat sPSF membrane (Fig. 3D, inset). Furthermore, the breakthrough time in the case of the 20 wt % PAF-1-SH membrane was approximately double that achieved with the 10 wt % membrane. Because of this high attainable efficiency, 1 kg of 20 wt % PAF-1-SH membrane material may treat up to 34,500 liters of water contaminated with 5 ppm Hg^{2+}

before regeneration is required (table S8), according to simplified upper-bound calculations (section 2.3 of the supplementary materials).

To test the generalizability of the IC-ED approach for the capture of diverse target ions, we also fabricated sPSF membranes embedded with particles of PAF-1-SMe (thioether) or PAF-1-ET (ether-thioether), which are selective for Cu^{2+} (18) and Fe^{3+} (23), respectively (section 1.1 of the supplementary materials). Notably, the resulting composite membranes are optically transparent (fig. S4), flexible (fig. S5), and dispersible (figs. S16 and S19) while also exhibiting polymer matrix compatibility (fig. S19 and table S3). Composite membranes containing 20 wt % of PAF-1-SMe or PAF-1-ET were tested in our IC-ED setup for the capture of Cu^{2+} or Fe^{3+} from feed solutions containing 6 ppm Cu^{2+} or 2.3 ppm Fe^{3+} , respectively, in 0.1 M HEPES buffer. The target ion concentration in each feed solution was reduced by the membranes to levels below detection with ICP-OES with no permeation into the receiving solution, and the membranes simultaneously achieved >96 to 99% desalination of their feeds (Fig. 4, A and B). As expected, negligible target ion capture was obtained when using neat sPSF membranes (figs. S47 and S48).

The fundamental insights from our IC-ED analyses can be applied more broadly to create other multifunctional membrane separation processes. For example, composite membranes prepared by incorporating PAF-1-NMDG (*N*-methyl-*D*-glucamine) (22) nanoparticles in sPSF (figs. S1, S4, and S5) were found to be highly selective for $\text{B}(\text{OH})_3$ capture in solute-capture diffusion dialysis (SC-DD) (fig. S33). In this process, concentration gradients, rather than electric potential gradients, drive solute transport across the membrane. Membranes containing 20 wt % PAF-1-NMDG selectively captured $\text{B}(\text{OH})_3$, reducing levels of the solute in the feed solution below levels detectable by ICP-OES, without any measured permeation into the receiving solution (Fig. 4C). By contrast, no appreciable $\text{B}(\text{OH})_3$ was captured by a neat sPSF membrane (Fig. 4C, inset). Notably, 20 wt % PAF-1-SH composite membranes also exhibited selective Hg^{2+} capture when used in our SC-DD setup (fig. S52). These results suggest that an array of efficient, multifunctional processes, such as IC-ED and SC-DD, can be developed through modification of traditional membrane processes (for example, for gas separations or fuel cells), regardless of the transport driving force.

We have described a general approach for the fabrication of robust, tunable adsorptive membranes through incorporation of PAF nanoparticles into ion exchange membranes. Implementation of these membranes in IC-ED and SC-DD processes enables exceptionally selective capture of target solutes [in this work, Hg^{2+} , Cu^{2+} , Fe^{3+} , and $\text{B}(\text{OH})_3$] and simultaneous

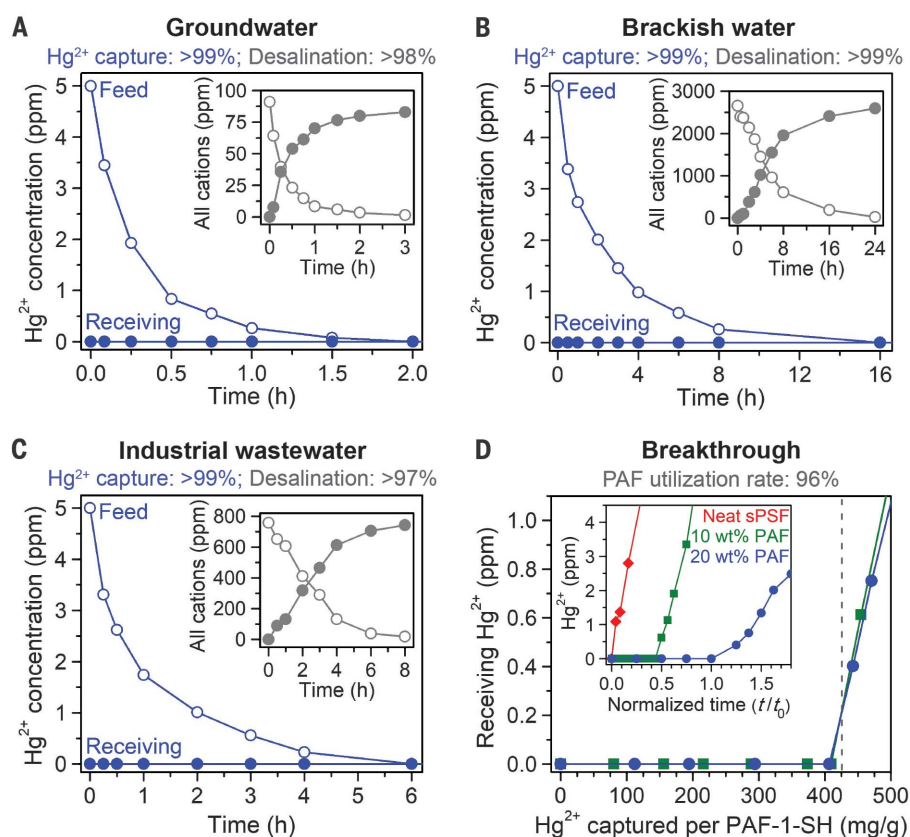


Fig. 3. IC-ED of diverse water sources. (A to C) Results from IC-ED of synthetic (A) groundwater, (B) brackish water, and (C) industrial wastewater containing 5 ppm Hg^{2+} by using 20 wt % PAF-1-SH in sPSF (applied voltage, -4 V versus Ag/AgCl). All Hg^{2+} was selectively captured from the feeds (open circles) without detectable permeation into the receiving solutions (solid circles). (Insets) All other cations were transported across the membranes to desalinate the feeds. The long duration of the IC-ED tests is an artifact of the experimental setup rather than the materials or IC-ED method (section 2.2 of the supplementary materials). (D) Breakthrough data for IC-ED using sPSF embedded with 10 or 20 wt % PAF-1-SH. Receiving Hg^{2+} concentrations are plotted against the amount of Hg^{2+} captured at different time intervals (in milligrams per gram of PAF-1-SH in each composite membrane). The predicted capacity (gray dotted line) corresponds to the Hg^{2+} uptake achieved by using PAF-1-SH powder under analogous testing conditions (section 1.10 of the supplementary materials). (Inset) Concentration of Hg^{2+} in the receiving solutions for IC-ED processes using neat sPSF (diamonds) and sPSF with 10 wt % PAF-1-SH (squares) and 20 wt % PAF-1-SH (circles), plotted versus time t normalized by the breakthrough time for the 20 wt % PAF-1-SH composite membrane, t_0 . Mean values determined from two replicate experiments are shown. Initial feed, 100 ppm Hg^{2+} in 0.1 M NaNO_3 ; applied voltage, -2 V versus Ag/AgCl .

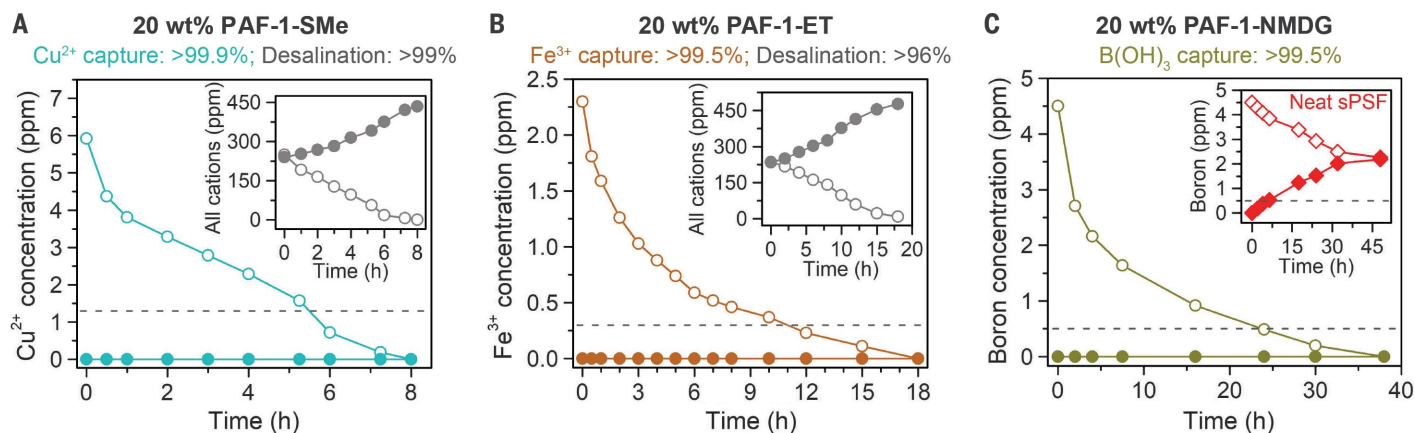


Fig. 4. Tuning membranes to selectively recover various target solutes.

(A and B) Cu^{2+} - (A) and Fe^{3+} -capture (B) electro dialysis (applied voltages, -2 and -1.5 V versus Ag/AgCl , respectively) using composite membranes with 20 wt % PAF-1-SMe and PAF-1-ET in sPSF, respectively. HEPES buffer (0.1 M) was used as the source water in each solution to supply competing ions and maintain constant pH. The insets show the successful transport of all competing cations across the membrane to desalinate the feed. (C) $\text{B}(\text{OH})_3$ -capture diffusion dialysis of groundwater containing 4.5 ppm boron using

composite membranes with 20 wt % PAF-1-NMDG in sPSF (no applied voltage). The inset shows results by using neat sPSF membranes for comparison. Open and solid symbols denote feed and receiving concentrations, respectively. Each plot point represents the mean value determined from two replicate experiments. Gray dotted lines indicate recommended maximum contaminant limits imposed by the US Environmental Protection Agency (EPA) for Cu^{2+} (29), the EPA and World Health Organization for Fe^{3+} (29, 30), and agricultural restrictions for sensitive crops for $\text{B}(\text{OH})_3$ (31).

desalination of diverse source waters. The high efficiency of this one-step process contrasts starkly with conventional intensive water treatment methodologies, which require multiple steps to achieve similar results (further comparisons are in section 2.5 of the supplementary materials) (28). The technology should be suitable more broadly for use with diverse adsorptive membranes and in the purification of complex water streams at various scales, such as in isolated regions that lack the necessary infrastructure for the treatment of contaminated groundwater or in desalination plants situated near nuclear waste sites for the treatment of wastewater polluted with radionuclides. To achieve these more complex separations, we envision the design of membranes featuring specialized combinations of embedded adsorbents, including nanoparticles of various hybrid and inorganic materials.

REFERENCES AND NOTES

- M. M. Mekonnen, A. Y. Hoekstra, *Sci. Adv.* **2**, e1500323 (2016).
- M. A. Shannon *et al.*, *Nature* **452**, 301–310 (2008).
- J. R. Werber, C. O. Osuji, M. Elimelech, *Nat. Rev. Mater.* **1**, 16018 (2016).
- M. R. Landsman *et al.*, *Annu. Rev. Chem. Biomol. Eng.* **11**, 559–585 (2020).
- D. S. Sholl, R. P. Lively, *Nature* **532**, 435–437 (2016).
- W. W. Li, H. Q. Yu, B. E. Rittmann, *Nature* **528**, 29–31 (2015).
- H. B. Park, J. Kamcev, L. M. Robeson, M. Elimelech, B. D. Freeman, *Science* **356**, eaab0530 (2017).
- J. R. Werber, A. Deshmukh, M. Elimelech, *Environ. Sci. Technol. Lett.* **3**, 112–120 (2016).
- S. Bolisetty, R. Mezzenga, *Nat. Nanotechnol.* **11**, 365–371 (2016).
- Y. Zhang *et al.*, *ACS Cent. Sci.* **4**, 1697–1707 (2018).
- K. V. Petrov, L. Paltrinieri, L. Poltorak, L. C. P. M. de Smet, E. J. R. Sudhölter, *Chem. Commun.* **56**, 5046–5049 (2020).

- S. Chaudhury, O. Nir, *Ind. Eng. Chem. Res.* **59**, 10595–10605 (2020).
- J. E. Bachman, Z. P. Smith, T. Li, T. Xu, J. R. Long, *Nat. Mater.* **15**, 845–849 (2016).
- T. Ben *et al.*, *Angew. Chem. Int. Ed.* **48**, 9457–9460 (2009).
- Y. Tian, G. Zhu, *Chem. Rev.* **120**, 8934–8986 (2020).
- B. Li, Y. Zhang, D. Ma, Z. Shi, S. Ma, *Nat. Commun.* **5**, 5537 (2014).
- S. Demir *et al.*, *ACS Cent. Sci.* **2**, 253–265 (2016).
- S. Lee *et al.*, *J. Am. Chem. Soc.* **138**, 7603–7609 (2016).
- Y. J. Yang *et al.*, *J. Mater. Chem. A* **6**, 5202–5207 (2018).
- Y. Yuan *et al.*, *Adv. Mater.* **30**, e1706507 (2018).
- B. Li *et al.*, *ACS Appl. Mater. Interfaces* **9**, 12511–12517 (2017).
- J. Kamcev *et al.*, *Adv. Mater.* **31**, e1808027 (2019).
- S. Lee *et al.*, *Chem. Sci.* **10**, 6651–6660 (2019).
- T. Ma *et al.*, *ACS Appl. Mater. Interfaces* **12**, 30474–30482 (2020).
- X. Li *et al.*, *Chem. Soc. Rev.* **46**, 7124–7144 (2017).
- S. J. D. Smith *et al.*, *Acc. Chem. Res.* **53**, 1381–1388 (2020).
- H. Fan, N. Y. Yip, *J. Membr. Sci.* **573**, 668–681 (2019).
- M. Elimelech, W. A. Phillip, *Science* **333**, 712–717 (2011).
- U.S. Environmental Protection Agency (EPA), “2018 edition of the drinking water standards and health advisories” (US EPA, 2018).
- World Health Organization, “Guidelines for drinking-water quality, 4th edition, incorporating the 1st addendum” (WHO, 2017).
- E. Güler, C. Kaya, N. Kabay, M. Arda, *Desalination* **356**, 85–93 (2015).

ACKNOWLEDGMENTS

We thank H. Furukawa for analysis of pore size distributions, T. Xu for assistance with dynamic light scattering measurements, N. P. Balsara for potentiostat use, J. Breen for fabrication of electro dialysis cells, D. J. Miller for assistance with water contact angle measurements, E. Kreimer and the Microanalytical Facility for microbalance use and assistance with elemental analyses and ICP-OES measurements, R. Kostecki and E. Velasquez for helpful discussions, and K. R. Meihaus for editorial assistance. **Funding:** The synthesis and characterization of materials and membranes were supported by the Center for Gas Separations, an Energy Frontier Research Center supported by the US Department of Energy (DOE), Office of Science, Office of Basic Energy Sciences

(award DE-SC0001015), and the electro dialysis measurements were supported by the US DOE, Office of Science, Office of Basic Energy Sciences (award number DE-SC0019992). Preliminary experiments were also supported by the Molecular Foundry and the Laboratory Directed Research and Development (LDRD) Program of the US DOE (contract no. DE-AC02-05CH11231) for Lawrence Berkeley National Laboratory. We thank the US National Science Foundation for providing graduate fellowship support for A.A.U. and M.K.T. We gratefully acknowledge the support of the Center for Integrated Nanotechnologies, an Office of Science User Facility operated for the US DOE Office of Science. Sandia National Laboratories is a multimission laboratory managed and operated by National Technology and Engineering Solutions of Sandia, LLC, a wholly owned subsidiary of Honeywell International, Inc., for the US DOE’s National Nuclear Security Administration (contract no. DE-NA-0003525). The views expressed in the article do not necessarily represent the views of the US DOE or the US government. **Author contributions:** A.A.U., J.J.U., and J.R.L. formulated the project with valuable input from N.T.B., J.K., and M.K.T.; A.A.U. synthesized the PAFs and membranes with assistance from J.K. and M.K.T.; A.A.U. performed and analyzed all material characterizations. A.A.U. collected and analyzed the adsorption data. A.A.U. and N.T.B. designed the electro dialysis cells. A.A.U. collected and analyzed the electro dialysis and diffusion dialysis data. N.T.B. performed and analyzed preliminary electro dialysis experiments and preliminary microscopy characterizations. A.A.U. and J.R.L. wrote the manuscript, and all authors contributed to revising the manuscript. **Competing interests:** The University of California, Berkeley, has applied for a patent (US application no. 63/079,457) on some of the technology discussed here, on which A.A.U., N.T.B., J.J.U., and J.R.L. are listed as coinventors, as well as an additional patent (US application no. 63/118,322) on some of the materials discussed here, on which A.A.U. and J.R.L. are listed as coinventors. **Data and materials availability:** All data are available in the manuscript or the supplementary materials.

SUPPLEMENTARY MATERIALS

science.sciencemag.org/content/372/6539/296/suppl/DC1
Materials and Methods
Supplementary Text
Figs. S1 to S59
Tables S1 to S8
References (32–71)

8 November 2020; accepted 15 March 2021
10.1126/science.abb5991

Ion-capture electrodialysis using multifunctional adsorptive membranes

Adam A. UlianaNgoc T. BuiJovan KamcevMercedes K. TaylorJeffrey J. UrbanJeffrey R. Long

Science, 372 (6539), • DOI: 10.1126/science.abf5991

One-step purification and desalination

The purification of water for drinking purposes can require multiple filtration steps and technologies to remove contaminants such as salts and heavy metals. Some contaminants could have value if recovered, but these are often discharged in the waste streams. Uliana *et al.* describe a general approach for the fabrication of robust, tunable, adsorptive membranes through the incorporation of porous aromatic framework (PAF) nanoparticles into ion exchange membranes such as those made from sulfonated polymers. Salts are removed using a series of cation and anion exchange membranes, and the PAF particles can be selected to capture specific target ions, such as those of copper, mercury, or iron. This allows for simultaneous desalination and decontamination of the water.

Science, this issue p. 296

View the article online

<https://www.science.org/doi/10.1126/science.abf5991>

Permissions

<https://www.science.org/help/reprints-and-permissions>

Use of think article is subject to the [Terms of service](#)

Science (ISSN 1095-9203) is published by the American Association for the Advancement of Science, 1200 New York Avenue NW, Washington, DC 20005. The title *Science* is a registered trademark of AAAS.

Copyright © 2021 The Authors, some rights reserved; exclusive licensee American Association for the Advancement of Science. No claim to original U.S. Government Works